

Emittance growth in recent antiproton transfers from Accumulator to Main Ring

F. M. Bieniosek
28-Sep-95

This note presents a study of emittance growth in pbar extractions from the Accumulator stack to circulating beam at 8 GeV in the Main Ring, for shots 5480 to 5629 (Apr 17, 1995 to July 23, 1995). During this period several bouts of large emittance blowups were encountered. Emittance of the beam extracted from the Accumulator directly affects collider luminosity. The motivation for this work is that if the sources of emittance growth can be found and corrected, significant increases in luminosity can be expected. Even in different operating scenarios, such as with the proposed Recycler ring, emittance growth must be understood and controlled to prevent pbar losses on transfer to the Recycler.

To help locate the source of the emittance growth, emittance growth is divided into two parts: first that which occurs during extraction from the stack to the beamline AP3, and second that due to injection into the Main Ring. SEMs in the beamline are used to determine the relative amounts of emittance growth in the two processes. Data for each individual transfer were collected for the study. For roughly half of these shots, SEM 900 (adjacent to the Accumulator) was inserted. SEM 105 is generally used as a day-to-day monitor of beam quality as the beam enters the Main Ring, but the beta functions are not independently well determined. Because the beta functions at SEM 900 are known as well as those in the Accumulator, only data from this SEM are used here. The data show that emittance growth occurs in each step of the process. More than half of the emittance growth occurs before the extracted beam enters the beamline.

In order to determine the beta functions at SEM 900, measurements of the beta functions in the Accumulator were made. Measurements were made in June and July of 1995 by measuring tune shift caused by varying eight quad shunts in the Accumulator. The local β -function at the varied quad is given by

$$\beta_{x,y} = 4\pi(B\rho)\frac{1}{S} \frac{dq_{x,y}}{di}$$

where $B\rho$ represents the momentum of the particle; S is the incremental strength of the quadrupole (in units of T/A), and dq/di is the slope of a curve fitted through the tune vs shunt current data. Accuracy of measuring the beta functions in this manner is estimated to be $\pm 25\%$. Data generally show reasonable agreement with a MAD model of the Accumulator lattice, with significant variation across the aperture only in the high-dispersion region (A4Q14). The measured beta functions are listed in Table 1 for “extraction” (628727 Hz), “central” (628870 Hz) and “core” (628955 Hz) orbits. Measurements on the extraction orbit may in some cases be distorted by strong coupling that splits the tune lines. In order to at least partially address this problem, in several cases, including the quads near the AP3 beamline (A2Q4 and A2Q5), the quoted numbers represent the average of two measurements with different settings on the skew quadrupoles.

Table 1
Measured beta functions in the Accumulator [m].

	horizontal			vertical		
	extraction	central	core	extraction	central	core
A2Q4	8.7	10.8	11.6	5.0	5.0	4.9
A1Q4	7.6	9.7	13.0	3.8	4.2	3.7
A2Q5	3.7	3.7	3.1	28.7	26.1	25.2
A1Q5	---	4.2	4.4	32.3	30.0	29.5
A1Q1	13.9	18.4	17.6	30.1	30.0	28.0
A5Q1	---	17.2	19.1	---	26.3	26.4
A3Q7	11.3	9.5	8.2	34.1	27.3	31.6
A3Q8	12.1	16.4	17.1	5.5	4.2	4.1
A4Q14	5.8	13.5	13.1	17.5	14.2	11.1

These results may be compared with an earlier measurement by the dipole trim method using two trim dipoles near the AP3 beamline. The displacement in the Accumulator is

$$\Delta x, y_{BPM} = \frac{\sqrt{\beta_d \beta_{BPM}}}{2 \sin \pi q_{x,y}} \theta_{x,y} \cos(\pi q_{x,y} - \Delta\phi)$$

where the β -functions are at the dipole and at the BPM; θ is the angle of deflection; q is the tune, and $\Delta\phi$ is the phase difference between dipole and BPM. For small $\Delta\phi$, the displacement becomes

$$\Delta x, y_{BPM} \cong \frac{1}{2} \sqrt{\beta_d \beta_{BPM}} \theta_{x,y} \cot \pi q_{x,y}$$

Averaging all the data from this measurement yields horizontal $\beta_x = \sqrt{\beta_d \beta_{BPM}} = 8.2$ m, vertical $\beta_y = \sqrt{\beta_d \beta_{BPM}} = 16.2$ m at trims and BPMs in the region between A2Q4 and A2Q5. These numbers are consistent with the quad measurements.

Extrapolating the measured lattice functions in the Accumulator at A2Q4 and A2Q5 yields $\beta_x = 18$ m; $\beta_y = 10$ m at SEM 900. For comparison, the nominal beamline model values for beta function are 22.5 m and 8.8 m respectively.

Figure 1 shows the transverse emittances in the stack prior to extraction. These measurements are based on measurements of the power in the sidebands of the transverse Schottky signals. Signal suppression due to the dampers causes the measured core emittances to be smaller than the actual core emittances. Hence there is some uncertainty in these measurements. This uncertainty impacts the measured emittance increase. Independent calibration of the emittance monitors would reduce the uncertainty.

Figure 2 summarizes the emittance data at the three locations: Accumulator, SEM 900, and the Main Ring. The data for emittance in the Accumulator and at SEM 900 are taken for each transfer. The data for Main Ring injection are shown for comparison, but they are older data from Stan Pruss's data base, averaged over 6 transfers of a shot. Note that emittance growth is predominantly vertical to SEM 900, but horizontal from there to the Main Ring. Some horizontally-large emittance points (>20 pi) have been clipped off this graph.

Figure 3 shows the averaged emittances at the core $\gamma(\epsilon_x + \epsilon_y)/2$ (red triangles) and the horizontal emittance (open circles) calculated from beam size at SEM 900. Emittances at the SEM are calculated by

$$\epsilon = \frac{6\gamma}{\beta} \left[\sigma^2 - \left(D \frac{\sigma_p}{p} \right)^2 \right]$$

where the value of β is based on the measurements above, D is taken from the beamline model, and σ_p / p is taken to be 6×10^{-4} . The emittances are multiplied by the relativistic factor γ to correspond with convention in the Main Ring. The horizontal emittance at SEM 900 is in some cases smaller than the horizontal emittance at the core; conversely the vertical emittance is much larger than vertical emittance at the core. To analyze the data, the assumption is made that strong coupling on the Accumulator extraction orbit couples the horizontal and vertical emittances while the beam is sitting on the extraction orbit prior to extraction - hence the average of the two values is used for comparison

with the beamline emittances. Unfortunately, horizontal emittance in the Main Ring is not directly available for comparison, since horizontal flying-wire data at injection were not considered to be reliable during the period of this study.

Figure 4 shows the horizontal emittance growth in the Accumulator (difference between the average core and SEM 900 emittances). There appear to be two or three classes of transfers: first, those with 0-5 π emittance growth, possibly split into two groups clustered around 1 π and 5 π emittance growth, and third, very large emittance growth, up to 30 π . It is likely that imperfections in the damper, or instabilities excited by the unstacking process, are involved in the large emittance-growth cases. These cases are often associated with “notches” and “spikes” in damper power and in (2-q, etc.) instability lines. The cases of fixed emittance growth to SEM 900 suggest another source of emittance growth.

Figure 5 shows the vertical emittance growth to SEM 900 ($\beta_y=10$ m; $D_y=0.5$ m). This plot shows growth (at least 1-4 π) for all of the transfers. The occasional large vertical-growth cases are usually associated with the large horizontal blowups. The vertical emittance growth is generally indicative of a problem in the Accumulator, which is unknown at present, and which needs to be addressed in detail.

Vertical data can be compared with Main Ring vertical flying-wire data on injection. Figure 6 shows the measured vertical emittances as a function of stack size. Triangles represent the Accumulator core, open circles SEM 900, and filled circles Main Ring injection. Emittance growth occurs at each step in the process. Plotting the data as a function of emittance at SEM 900 (figure 7) shows more clearly the emittance growth occurring in the Accumulator. Vertical emittance increases by a factor of 2-4 between the average core emittance and SEM 900. Vertical emittance on injection into the Main Ring clusters slightly above the emittance at SEM 900 (solid line); the additional emittance increase is roughly 2-3 π .

Transfer efficiency to the Main Ring at 8 GeV (fig. 8) correlates well with the average transverse emittance at SEM 900. The curve is a Gauss fit to the data. Correlation is much better than for other parameterizations (Main Ring vertical emittance, horizontal or vertical emittance at the SEM), indicating that horizontal and vertical emittances are both significant to transfer efficiency.

There are several sources of emittance growth on injection into the Main Ring. Growth estimates are as follows. [1]

1. Transverse injection oscillations lead to an emittance increase of

$$\Delta\varepsilon = 6 \left(\frac{\pi}{2} \right) \frac{(\Delta x)^2}{\beta}$$

where β is the lattice amplitude function at the point of measurement. Typical injection oscillations are 1-2 mm in each plane. A 2-mm injection oscillation leads to a $1.1\text{-}\pi$ emittance growth assuming $\beta = 100$ m.

2. Scattering at SEMs in the beamline causes an emittance increase of

$$\Delta\varepsilon = 6\left(\frac{\pi}{2}\right)\beta(\Delta\theta)^2$$

where $\Delta\theta$ is the scattering angle through the SEM foil. Typical estimates for emittance increase are in the range of 0.3π (SEM 105) to 1.3π (SEM 103).

3. Amplitude function mismatch can lead to an emittance increase. The effect is probably not large vertically, because the slope of Main Ring emittance plotted as a function of beamline emittance is about one. Emittance growth on transfer to the Main Ring may be estimated from the expression

$$F = \frac{1}{2}\left(\beta\gamma_0 + \beta_0\gamma - 2\alpha\alpha_0\right)$$

where the unsubscripted Courant-Snyder parameters are those delivered by the beamline to the Main Ring, and the subscripted parameters are the periodic Main Ring lattice functions at the end of the beamline. The function F represents the relative emittance growth of the injected beam $\varepsilon/\varepsilon_0$ if the mismatch is not too large. Modelling the beamline to determine the final match to the Main Ring is difficult because of uncertainty in magnet strengths. Small errors are cumulative over the length of the line, making the ultimate beam conditions difficult to accurately pin down. The task of modelling the beamline and magnets is an on-going effort, and will be the subject of a separate write-up, when completed. The current TRANSPORT model indicates that mismatch is small: $F = 1.08$ horizontally, and 1.14 vertically. A small mismatch agrees with the vertical data; it would be interesting to measure horizontal emittance growth on injection into the Main Ring to verify the TRANSPORT result horizontally as well.

4 Dispersion mismatch to the Main Ring can cause an emittance increase. Measurements were made of the dispersion mismatch by injecting off-momentum bunches separated by 10 Hz, corresponding to $\Delta p/p = 6.92 \times 10^{-4}$. The resulting transverse oscillations in the difference orbit in the Main Ring depend on the dispersion.

$$\Delta x = D_x \frac{\Delta p}{p}$$

Figure 9 shows horizontal dispersion (synch model) in the Main Ring for a circulating beam (solid curve), and dispersions calculated from measured first-turn displacements of

injected pbars for three beamline tunes. The difference between the data and the solid curve represents the dispersion mismatch. The original dispersion mismatch (10/27/94) was about 8 m. After two improvements in the match, the dispersion match was improved significantly. However the fit of 1/27/95 had poor transfer efficiency, presumably due to amplitude-function mismatch, and was abandoned. The result is that the current horizontal dispersion mismatch (measured 12/14/94) is about 4.5 m. This corresponds roughly to an emittance growth of about 2π . Vertical dispersion mismatch (Fig. 10) is smaller than horizontal mismatch (about 2 m), with emittance growth in the range of 0.5π .

In conclusion, a surprisingly large amount of emittance growth seems to take place in the Accumulator. The emittance growth in the Accumulator is not understood, and it may not even be well-quantified, due to uncertainties in core emittance. Further investigation is necessary. The small level of vertical emittance growth during Main Ring injection is consistent with known processes. Horizontal emittance growth during Main Ring injection is not well measured, but it is likely that some improvement could be made by further improving the horizontal dispersion function match.

[1] D. A. Edwards and M. J. Syphers, An Introduction to the Physics of High Energy Accelerators, Wiley, 1993.

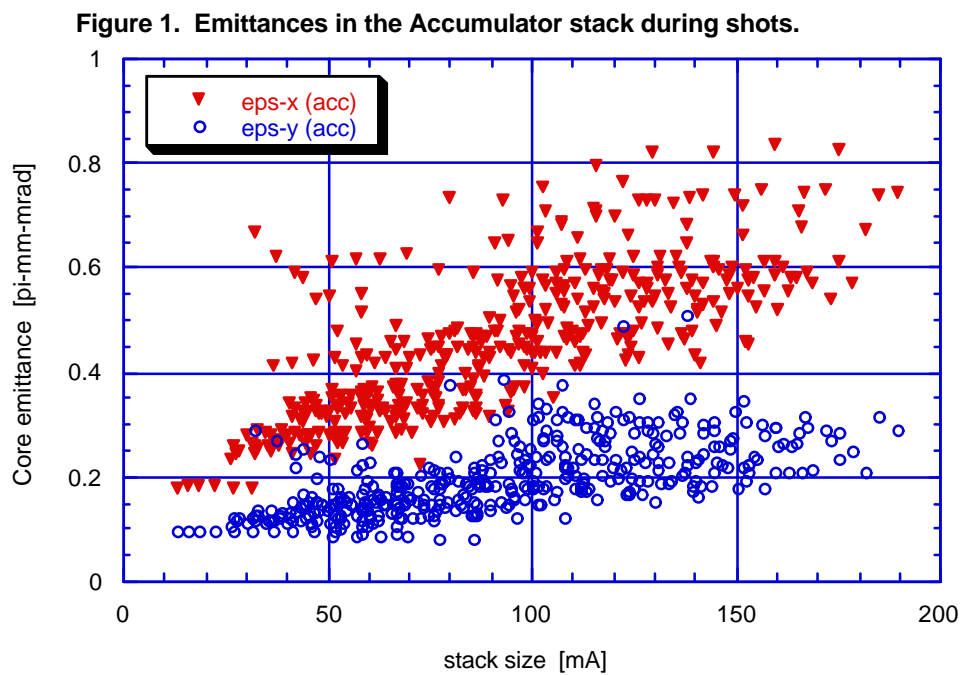


Figure 2. Horizontal vs vertical emittance in pbar transfers

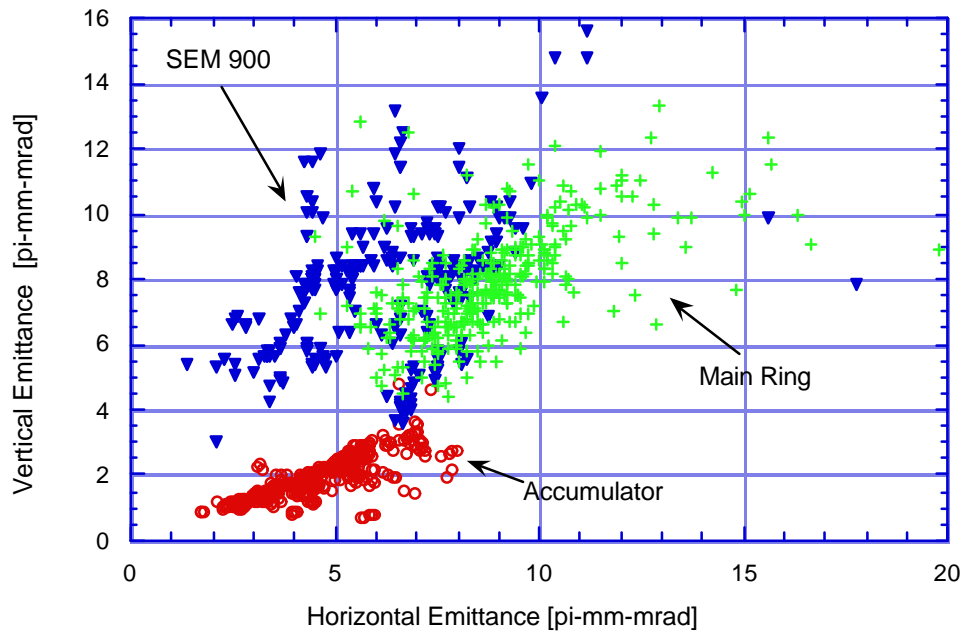


Figure 3. Horizontal emittances on transfers.

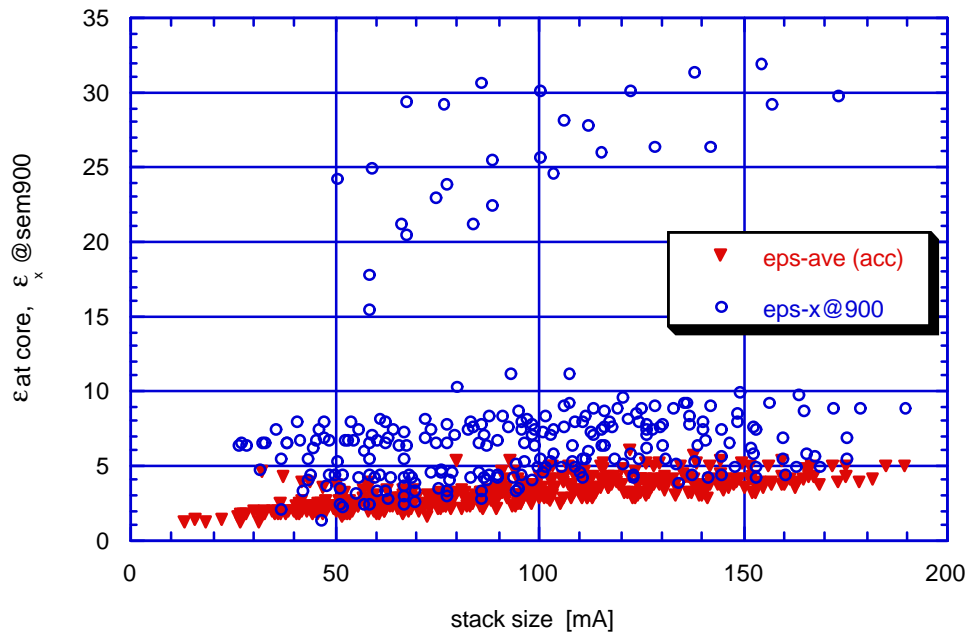


Figure 4. Horizontal emittance growth to SEM 900.

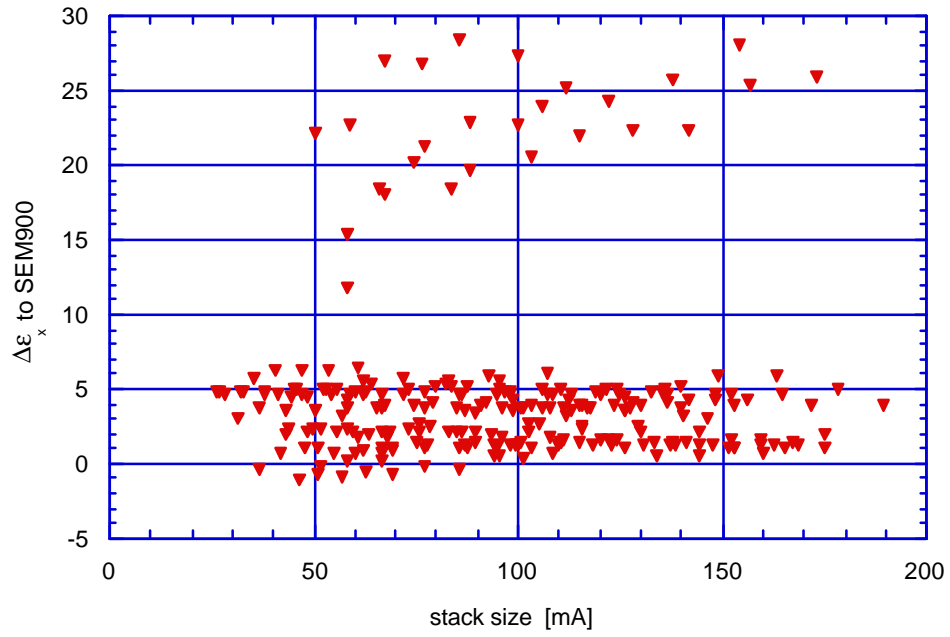


Figure 5. Vertical emittance growth to SEM 900.

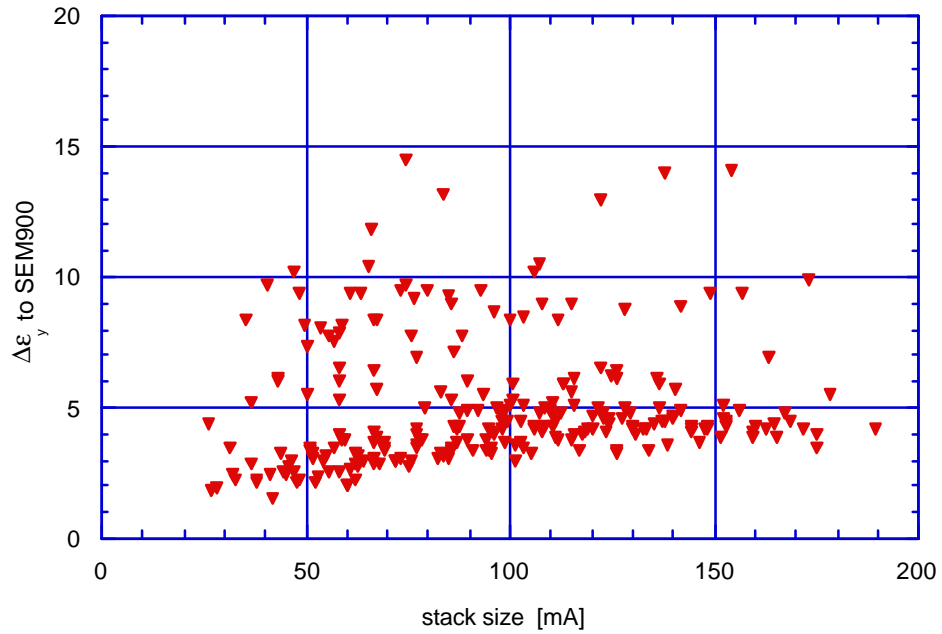


Figure 6. Vertical emittance at various stages in the transfer
- vs stack size.

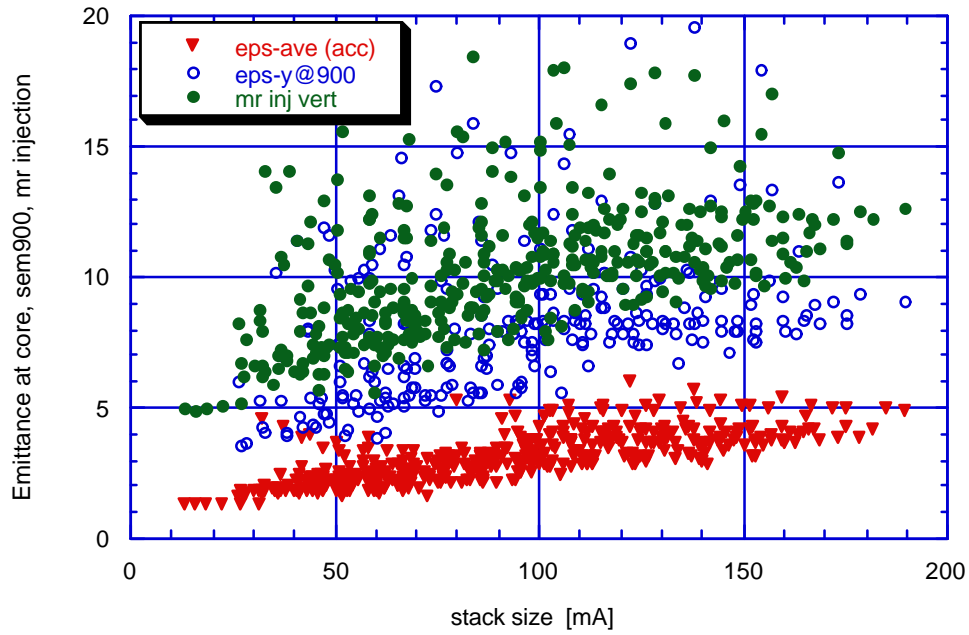


Figure 7. Vertical emittance at various stages in the transfer
- vs SEM 900.

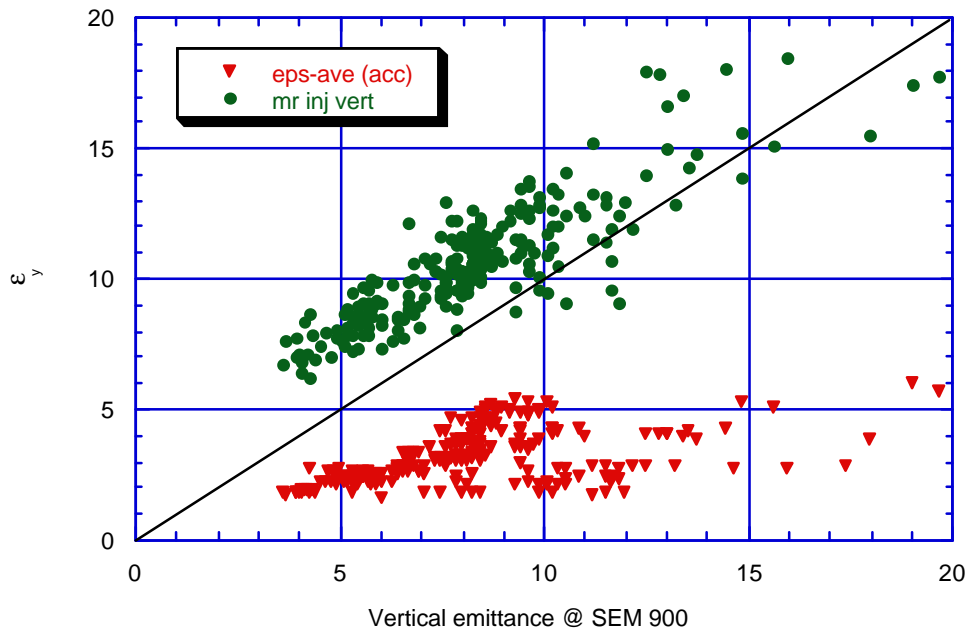


Figure 8. Dependence of transfer efficiency to Main Ring 8GeV on averaged transverse emittance at SEM 900.

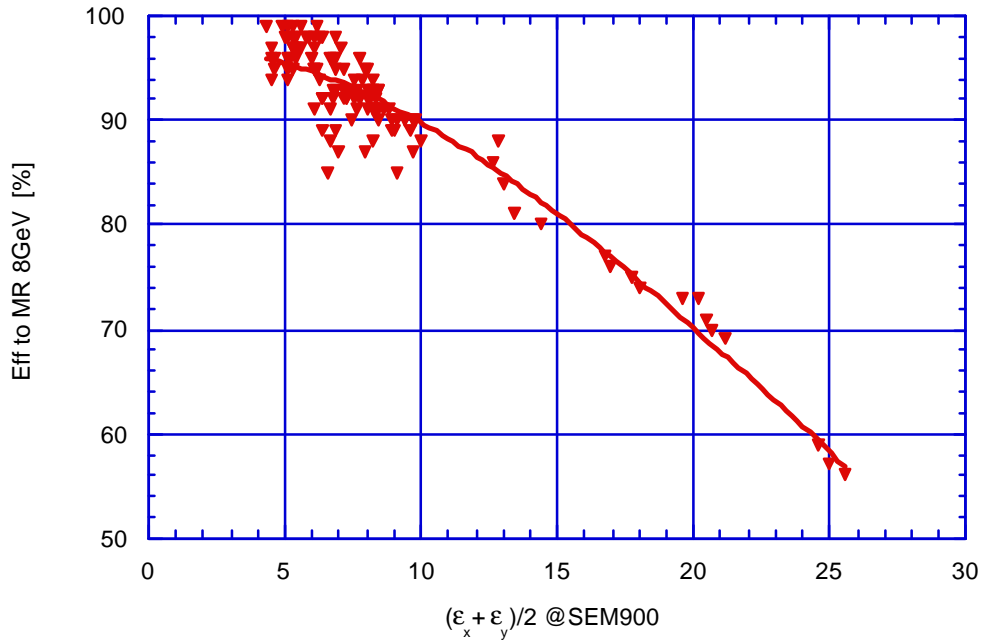


Fig 9. Horizontal dispersion in MR on test shots.

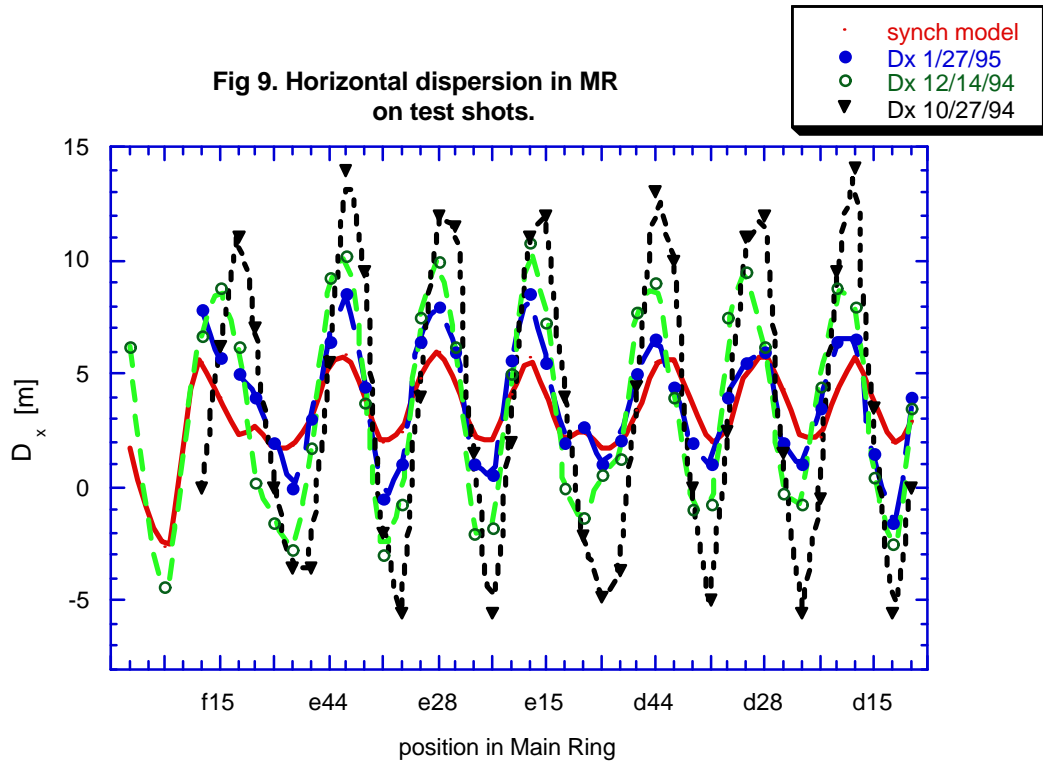


Fig 10. Vertical dispersion in MR on test shots.

